Electric-field-induced transition between ferro- and antiferroelectric ground states observed in the B7 phase of a bent-shaped molecule with alkylthio tails

Seng Kue Lee,* Xiaodong Li, Sungmin Kang, Masatoshi Tokita and Junji Watanabe

Received 24th December 2009, Accepted 8th February 2010
First published as an Advance Article on the web 8th March 2010
DOI: 10.1039/b927280a

We prepared a new bent-shaped molecule, in which dodecylthio tails and typical Schiff-based side wings are substituted on a conventional phenyl central core. This molecule forms the B7 phase in a temperature region from 117 to 142 °C, which shows characteristic banana leaf and circular domain textures. On application of an electric field, the B7 phase is easily transformed to the B2 phase with two different ground states, depending on the temperature. In the higher temperature region, the B2 phase possesses a homochiral ferroelectric (SmC_SP_F) ground state, whereas the lower temperature B2 phase has a homochiral antiferroelectric (SmC_AP_A) ground state. These two states transformed into each other reversibly at 124 °C under the applied field, while they are stable over the mesophase temperature on the field-off state.

Introduction

Since their discovery by Watanabe *et al.*,[1] bent-shaped (or banana) molecules and their unconventional mesophases with unique polarity[1] and chirality[2] have intrigued scientists and opened a new era in soft materials. The most interesting phenomenon of bent-shaped molecules is the occurrence of polar order and chiral properties from achiral molecules. Various examinations of ferro- and antiferroelectric behaviour, macroscopic chirality and optical activity have been performed for a large number of molecules, and at least eight different banana phases have been identified.[3–5]

Among these phases, the most extensively investigated phase is the B2 phase. Since the bent-shaped molecules in the B2 phase are tilted to the smectic layer, four distinct types of structures—homochiral (SmC_SP_F and SmC_AP_A) and racemic (SmC_SP_A and SmC_AP_F)—can be distinguished depending on the tilt and polar directions of the molecules in adjacent layers. The antiferroelectric state is generally the ground state. Moreover, depending on the switching current and optical microscopy measurements, most exhibit the synclinic antiferroelectric state (SmC_SP_A) as a ground state because of interlayer steric interaction. The structure satisfies the condition that the end chains in adjacent layers are parallel. This state is racemic, hence the chirality alters from layer to layer. Homochiral antiferroelectric (SmC_AP_A) order is less frequently observed, and a few ferroelectric ground states have been reported.[6–13]

The B7 phase has also been extensively studied because of its unique and characteristic textures, these include spiral, myelinic-like, accordion-like, checker-board-like, banana-leaf-like and circular domain textures.[14–18] From the electro-optical response and polarization reversal current measurements, B7 phases are thought to be ferroelectric, at least after application of an electric field.[14,16,19] In some cases, ferroelectric-like switching in the higher temperature region of the B7 phase changes to tristable switching with a decrease in temperature.[14,20] However, the details of the transformation are not described. The X-ray pattern is also characteristic of the B7 phase. It includes several sharp reflections in a small angle region and a broad diffuse scattering in a wide angle region, suggesting 2D ordered modulated structures, which are different from those in the B1 phases.[21]

In this study, we examined the electro-optical measurements for the B7-like phase of 1,3-phenylene bis[4-(4-dodecylsulfanylphenyliminomethyl)]benzoate,

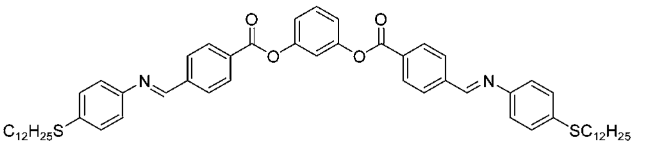

where the dodecylthio tails and typical Schiff-based side wings are substituted on a conventional phenyl central core. The B7 phase appears with the typical banana-leaf and circular domain textures, and exhibits a ferroelectric response. However, on cycling the temperature under an applied electric field, a clear transition occurs between the lower temperature antiferroelectric (SmC_AP_A) and higher temperature ferroelectric (SmC_SP_F) phases.

Experimental section

Measurements

The textures were observed under a crossed polarizer using an Olympus BX50 polarizing optical microscope (POM) equipped with a temperature controlled Mettler Toledo FP 90 hot stage. Transition temperatures were determined by differential scanning calorimetry (DSC) using a Perkin-Elmer DSC 7 calorimeter. The electro-optical response and polarization reversal current were observed with a high-speed voltage amplifier (FLC Electronics, F20A) connected to a function generator (NF Electronic Instruments, WF1945A). To eliminate the effects of electric field

Department of Organic and Polymeric Materials, Tokyo Institute of Technology, 2-12-1, O-okayama, Meguro-ku, Tokyo, 152-8552, Japan

strength, it was fixed at ±7.1 V μm^{-1} through all experimental processes. X-Ray diffraction measurements were performed using a Rigaku-Rint-2000 diffraction with Cu-Kα radiation.

Synthesis of 1,3-phenylene bis[4-(4-dodecylsulfanylphenyliminomethyl)]benzoate

A solution of phenylene 1,3-bis(4-formylbenzoate) (0.30 g, 0.80 mmol) and 4-dodecylsulfanylphenylamine (0.51 g, 1.76 mmol) in chloroform (20 ml) was heated under reflux for 3 h. The reaction mixture was concentrated and recrystallized from chloroform–ethanol to give 0.62 g, (83%) of 1,3-phenylene bis[4-(4-dodecylsulfanylphenyliminomethyl)]benzoate as yellow crystals. The preparation of the intermediate compounds was performed using procedures described in the previous report.[22] ^{1}H-NMR (400 MHz, $CDCl_3$) δ 0.88 (t, J = 6.8 Hz, 6 H), 1.25–1.68 (m, 40 H), 2.94 (t, J = 6.8 Hz, 4 H), 7.21–7.54 (m, 12 H), 8.04 (d, J = 8.4 Hz, 4 H), 8.30 (d, J = 8.4 Hz, 4 H), 8.57 (s, 2 H). Elemental analysis: calculated for $C_{58}H_{72}N_2O_4S_2$ C 75.28, H 7.84, N 3.03, O 6.92, S 6.93; found, C 74.96, H 7.92, N 2.70, O(+S) 14.42.

Results and discussion

The differential scanning calorimetry (DSC) thermogram is shown in Fig. 1. Two main peaks with ΔH = 35.1 kJ mol^{-1} (or 38.5 kJ mol^{-1}) and ΔH = 19.1 kJ mol^{-1} (or 20.3 kJ mol^{-1}) can be detected at 127 °C (or 117 °C) and 146 °C (or 141 °C), respectively, on heating (or cooling); these are attributable to crystal-B7 and B7-isotropic phase transitions.

The B7 phase was identified from microscopic observation of banana-leaf-like and circular domain textures in Fig. 2, although the screw-like helical domain characteristics of the B7 phase were not observed. From the circular domain, we know that the extinction directions are parallel and perpendicular to the layer normal. The X-ray pattern shows the simple layer structure with an outer broad reflection and inner layer reflection with spacing of around 4.5 Å and 45.9 Å, respectively. No additional reflections suggesting smectic layer undulations were observed.[21] The measured layer spacing is smaller than the molecule length of 54.4 Å, which was determined for the molecule with the most stable twist conformation of the central core and the most extended flexible tail chain. The tilt angle of the molecule to the layer was calculated as 32.5°.

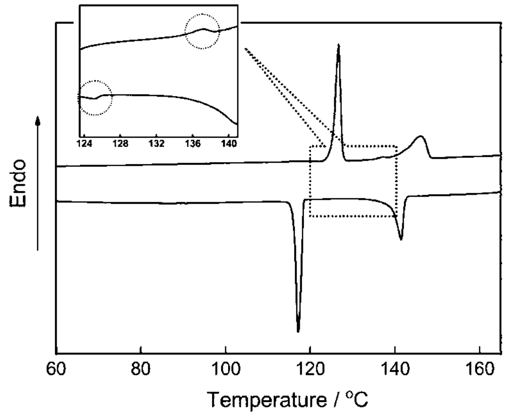

Fig. 1 DSC thermogram for heating and cooling cycles. Between the two main peaks, *i.e.*, within the B7 phase zone, a small, but significant peak can be identified from the enlarged view in the inset.

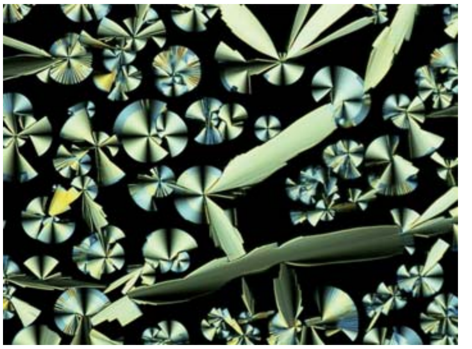

Fig. 2 Banana-leaf-like and circular domain textures of the B7 phase appearing from the isotropic melt.

By careful observation of the DSC curve, on heating, a small but significant peak with ΔH less than 0.3 kJ mol^{-1} is observed at 137 °C between the two previously mentioned peaks (see the enlarged view in the inset of Fig. 1). On cooling, the corresponding transition appears at 125 °C. Nothing is detected in the microscopic and X-ray observations at this small DSC transition. Thus, this small transition is due to a small structural change, which surely occurs in the B7 phase, although it is remarkably supercooled or superheated.

The present B7-like phase shows the characteristic switching behaviour against an external electric field. First, we applied an electric field for the B7 phase at a temperature that was a few degrees lower than the iso-B7 transition. Immediately after applying an electric field, a high-birefringent smooth fan-shaped texture was well developed with the extinction directions tilted to the polarizers. On reversing the field, the extinction direction of the fan-shaped domains rotates in the opposite direction and in the off-state of the electric field the extinction direction is retained, showing a ferroelectric response (Fig. 3a). The extinction direction from the polarizer axis is around 30°, which corresponds to the tilt angle of molecules to the layer as shown by X-ray spacing data. This ferroelectric behaviour is also ensured from a single switching current peak in a triangular wave field (Fig. 3b). Thus, the field-induced ground state is a bistable ferroelectric, with switching occurring between two homochiral ferroelectric (SmC_SP_F) states, as schematically illustrated in Fig. 4a. Of research interest is the alteration of switching behaviour when the temperature is decreased below 124 °C, although the fan-shaped texture remains unchanged. From microscopic observation, on reversing the field, the alternative rotation of extinction directions is invariably observed, but in the field off-state, their directions turn to correspond with the polarizer directions (Fig. 3c). Further, double switching current peaks are observed in a half circle of a triangular-wave electric field, as shown in Fig. 3d. This is typical antiferroelectric switching, where the ground state is SmC_AP_A and electro-optical switching takes place to the SmC_SP_F, as illustrated in Fig. 4b. This field-induced transformation between ferroelectric and antiferroelectric ground states is reversible on heating and cooling cycles as long as the electric field is applied. The transition temperature is around 124 °C, and is invariably detected

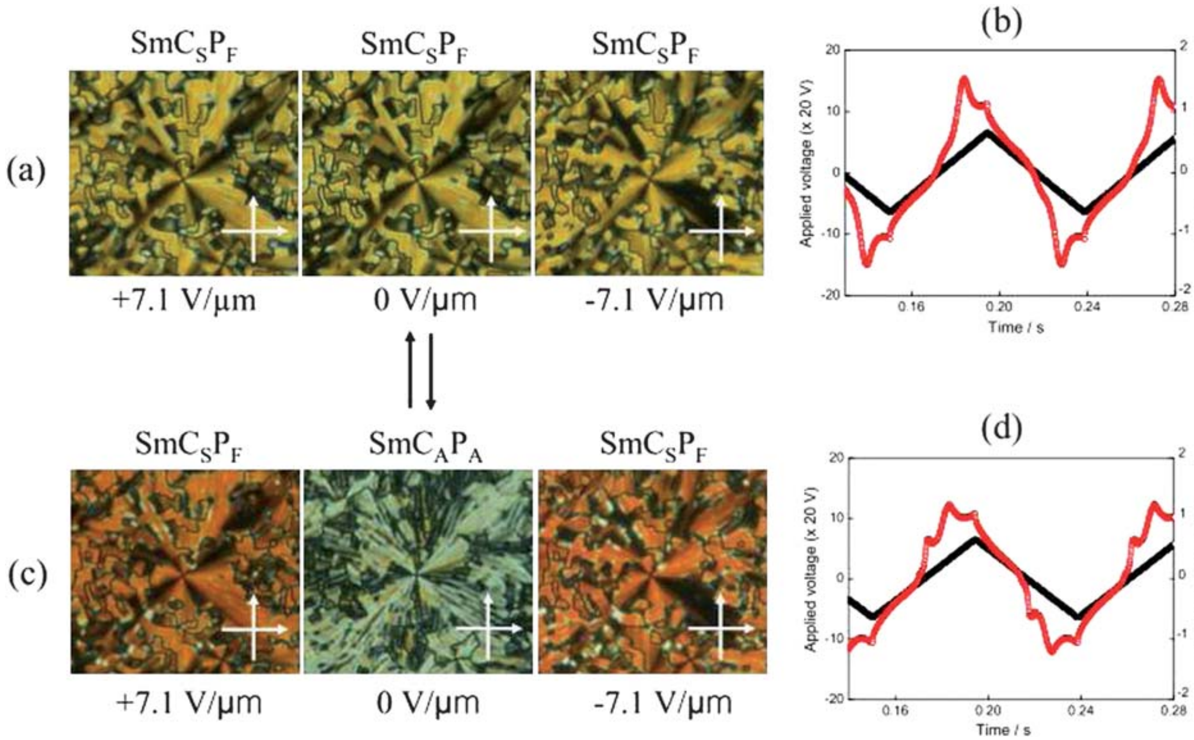

Fig. 3 Photomicrographs (a and c) and polarization reversal currents (b and d) observed upon application of the electric field: (a) and (b) at 130 °C, and (c) and (d) at 120 °C. At temperatures higher than 124 °C, optical microscopic textures in (a) indicate ferroelectric switching with a homochiral synclinic ferroelectric (SmC_SP_F) ground state. Ferroelectric switching is also supported by a single switching current peak on application of a triangular wave field (260 Vpp, 12 Hz) in (b). At temperatures below 124 °C, the ground state is altered to homochiral anticlinic antiferroelectric (SmC_AP_A) as found from the textural change in (c) and antiferroelectric switching is confirmed by the observation of two switching peaks in (d). This field-induced transformation between ferroelectric and antiferroelectric ground states is completely reversible in heating and cooling cycles as long as the electric field is applied.

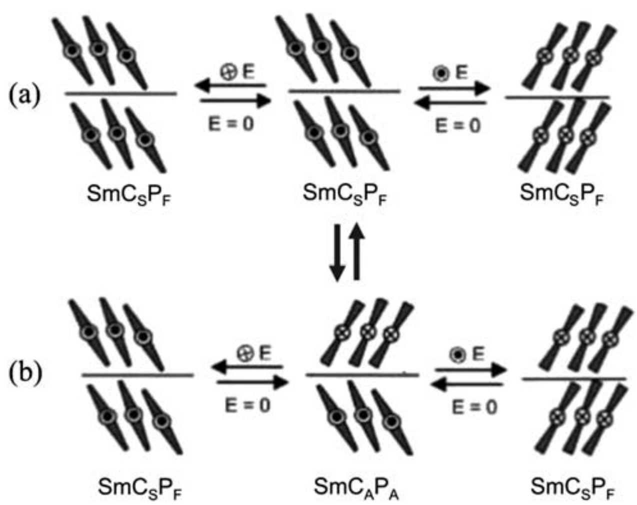

Fig. 4 Schematic representation of the molecular rearrangement on (a) ferroelectric switching in the higher temperature region and (b) antiferroelectric switching at lower temperatures.

during heating and cooling processes. In the field off-state, the field-induced ground state texture is retained on heating and cooling, even if the temperature is varied in the B7 temperature region. In other words, the ferro- or antiferroelectric ground state is very stable once it is induced by an electric field.

Here, two distinct features are extracted for the present B7 phase. First, the B7 phase is easily altered to the homochiral B2 phase by an electric field. This is because the B7 phase has a similar packing structure to the B2 phase in local space, and differs only by having a polarization-modulated structure.[21] In other words, the B7 structure escapes from a macroscopic polar order by a polarization splay that breaks the long layer correlation. Thus, the B7 phase possesses a 2D structure, which results in additional inner reflections in the X-ray pattern.[21] In the present B7 phase, only one inner reflection is detected, as in the B2 phase, although undulation may be likely since the extinction direction in the microscopic texture corresponds to the polarizer directions, irrespective of significant tilting of molecules to the layer. The undulation period may be too long to be detected by X-ray, and this long period may be attributable to the easy transformation of B7 into B2 on application of the electric field.

The second feature is that the field-induced ground state of the B2 phase in the higher temperature region is SmC_SP_F, while it is SmC_AP_A in the lower temperature region (Fig. 4). The difference is seen only in the clinicity, which can be produced by a small energy difference. The temperature (125 °C) of the small DSC peak observed on cooling the B7 phase corresponds to 124 °C of the field-induced transformation between the ferro- and antiferroelectric B2 phase. Thus, the small DSC peak can be attributed to the transition between the two ground states. The energy difference between the two states is 0.3 kcal mol^{-1}; such a small difference can be caused by the difference in the conformation of the alkylthio terminal chains[22] or the interaction of the terminal chains between the neighbouring layers. Here, the question arises as to why the transition does not take place for the field-induced B2 phase, but does so reversibly for the B7 phase. We speculate that there is an easier transformation process in the B7 phase because of its polarization modulation structure.

In summary, we prepared a bent-shaped molecule, in which the dodecylthio tails and typical Schiff-based side wings are substituted on a conventional phenyl central core. This molecule forms the B7 in the temperature region from 117 to 142 °C, which shows the characteristic banana leaf and circular domain textures, but is easily transformed to the B2 phase with a fan-shaped texture by application of an electric field. The electric-field-induced B2 phase appears with different ground states, depending on the temperature. At higher temperatures, the B2 phase possesses a ferroelectric (SmC_SP_F) ground state, whereas at lower temperatures the B2 phase shows an antiferroelectric (SmC_AP_A) ground state. These two states transformed into each other reversibly at 124 °C under the applied field, while they are stable over the mesophase temperature in the field-off state.

Acknowledgements

This research was supported by a Grant-in-Aid for Creative Scientific Research and a Grant-in-Aid for Young Scientists B (21750138) from the Ministry of Education, Culture, Sports, Science and Technology in Japan.

References

1 T. Niori, T. Sekine, J. Watanabe, T. Furukawa and H. Takezoe, *J. Mater. Chem.*, 1996, **6**, 1231.
2 D. R. Link, G. Natale, R. Shao, J. E. Maclennan, N. A. Clark, E. Korblova and D. M. Walba, *Science*, 1997, **278**, 1924.
3 G. Pelzl, S. Diele and W. Weissflog, *Adv. Mater.*, 1999, **11**, 707.
4 H. Takezoe and Y. Takanishi, *Jpn. J. Appl. Phys.*, 2006, **45**, 597.
5 R. A. Reddy and C. Tschierske, *J. Mater. Chem.*, 2006, **16**, 907.
6 D. A. Olson, M. Veun, A. Cady, M. V. D'agostino, P. M. Johnson, H. T. Nguyen, L. C. Chen and C. C. Huang, *Phys. Rev. E: Stat., Nonlinear, Soft Matter Phys.*, 2001, **63**, 041702.
7 C. Keith, R. A. Reddy, H. H. Lang and C. Tschierske, *Chem. Commun.*, 2004, 1898.
8 G. Dantgraber, A. Eremin, S. Diele, A. Hauser, H. Kresse, G. Pelzl and C. Tschierske, *Angew. Chem., Int. Ed.*, 2002, **41**, 2408.
9 H. Nadasi, W. Weissflog, A. Eremin, G. Pelzl, S. Diele, B. Das and S. Grande, *J. Mater. Chem.*, 2002, **12**, 1316.
10 J. P. Bedel, J. C. Rouillon, J. P. Maroerou, M. Lauerre, H. T. Nguyen and M. F. Achard, *Liq. Cryst.*, 2001, **28**, 1285.
11 R. A. Reddy and B. K. Sadashiva, *J. Mater. Chem.*, 2002, **12**, 2627.
12 R. A. Reddy, M. W. Schroder, M. Boddyagin, H. Kresse, S. Diele, G. Pezel and W. Weissflog, *Angew. Chem., Int. Ed.*, 2005, **44**, 774.
13 R. A. Reddy and B. K. Sadashiva, *J. Mater. Chem.*, 2004, **14**, 1936.
14 G. Pelzl, D. Diele, A. Jakli, C. H. Lischka, I. Wirth and W. Weissflog, *Liq. Cryst.*, 1999, **26**, 135.
15 J. Thisayukta, T. Sekine, Y. Nakayama and J. Watanabe, *Liq. Cryst.*, 2000, **27**, 1129.
16 J. P. Bedel, J. C. Rouillon, J. P. Marcerou, M. Laguerre, H. T. Nguyen and M. F. Achard, *J. Mater. Chem.*, 2002, **12**, 2214.
17 H. N. S. Murthy and B. K. Sadashiva, *Liq. Cryst.*, 2003, **30**, 1051.
18 P. Pyc, J. Mieczkowski, D. Pociecha, E. Gorecka, B. Donnio and D. Guillon, *J. Mater. Chem.*, 2004, **14**, 2374.
19 M. Nakata, D. R. Link, Y. Takanishi, Y. Takahasi, J. Thisayukta, H. Niwano, D. A. Coleman, J. Watanabe, A. Iida, N. A. Clark and H. Takezoe, *Phys. Rev. E: Stat., Nonlinear, Soft Matter Phys.*, 2005, **71**, 011705.
20 G. Pelzl, M. G. Tamba, S. F-Tandel, M. W. Scroder, U. Baumeister, S. Diele and W. Weissflog, *J. Mater. Chem.*, 2008, **18**, 3017.
21 D. A. Coleman, J. Fernsler, N. Chattham, M. Nakata, Y. Takanishi, E. Körblova, D. R. Link, R.-F. Shao, W. G. Jang, J. E. Maclennan, O. Mondainn-Monval, C. Boyer, W. Weissflog, G. Pelzl, L.-C. Chien, J. Zasadzinski, J. Watanabe, D. M. Walba, H. Takezoe and N. A. Clark, *Science*, 2003, **301**, 1204.
22 X. Li, S. K. Lee, S. Kang, M. Tokita, S. Kawauchi and J. Watanabe, *Chem. Lett.*, 2009, **38**, 424.

